

DNAzyme Footprinting: Detecting Protein–Aptamer Complexation on Surfaces by Blocking DNAzyme Cleavage Activity

Yulin Chen and Robert M. Corn*

Department of Chemistry, University of California—Irvine, Irvine, California 92697, United States

S Supporting Information

ABSTRACT: A novel method to quantitatively measure the binding of proteins to single-stranded DNA (ssDNA) aptamers that employs the inhibition of the DNAzyme hydrolysis of aptamer monolayers is described. A 28-base DNAzyme was designed to specifically bind to and cleave a 29-base ssDNA sequence that can fold into a G-quartet aptamer and bind the protein thrombin. The binding strength of the DNAzyme to the aptamer sequence was designed to be less than the binding strength of the thrombin to the aptamer ($\Delta G^\circ = -43.1$ and -51.8 kJ/mol, respectively). Formation of the thrombin–aptamer complex was found to block DNAzyme cleavage activity both in solution and in an ssDNA aptamer monolayer. We denote this method for detecting protein–aptamer complexation as “DNAzyme footprinting” in analogy to the process of DNase footprinting for the detection of protein–DNA interactions. By attaching a 40-base reporter sequence to the ssDNA aptamer monolayer, the detection of any protein–aptamer complexes remaining on the surface after DNAzyme activity can be greatly enhanced (down to one thrombin–aptamer complex per 10 000 ssDNA molecules corresponding to 100 fM thrombin in solution) by a subsequent surface RNA transcription amplification reaction followed by RNA detection with nanoparticle-enhanced SPR imaging. In addition to RNA transcription, DNAzyme footprinting can be coupled to a wide variety of other nucleic acid surface amplification schemes and thus is a powerful new route for the enzymatically amplified detection of proteins via protein–aptamer complex formation.

The development of novel surface bioaffinity methods to detect protein biomarkers at extremely low (subpicomolar) concentrations is crucial for the early stage clinical detection of a variety of infectious diseases, cancers, and neurological disorders.^{1–4} Surface bioaffinity measurements that employ DNA or RNA aptamers in lieu of antibody microarrays have recently emerged as a rapid and robust alternative for the detection of protein biomarkers in biological samples.^{5–7} Aptamers possess several potential advantages over antibodies for bioaffinity sensing: better air stability and shelf life, ease of fabrication, and reduced cross-reactivity via nonspecific adsorption.^{7,8} We have previously employed DNA and RNA aptamer microarrays for the direct detection of protein biomarkers with the techniques of surface plasmon resonance imaging (SPRI) and SPR phase imaging (SPR-PI) at

concentrations as low as 100 pM.^{9,10} In this letter, we demonstrate a novel method for the ultrasensitive detection of protein biomarkers that uses DNAzymes to recognize the specific adsorption of proteins onto aptamer monolayers. This methodology can be used in conjunction with both nanoparticle-enhanced SPRI (NE-SPRI)^{10–12} and enzymatically amplified SPRI^{6,13,14} to detect protein biomarkers from nanomolar to subpicomolar concentrations.

The key concept of this new method for the ultrasensitive detection of proteins with aptamer monolayers is the use of surface bound protein–aptamer complexes to block the site-specific nucleic acid cleavage activity of DNAzymes. We label this process “DNAzyme footprinting”, and Figure 1 shows how

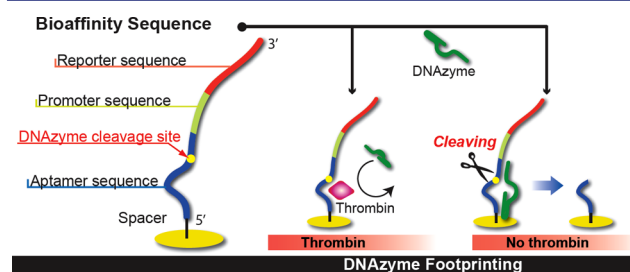


Figure 1. Schematic diagram of the DNAzyme footprinting methodology.

we use this concept. DNAzyme footprinting requires two components: (i) a single-stranded DNA (ssDNA) molecule that we denote as the “bioaffinity sequence” that can reversibly fold into an aptamer structure and noncovalently bind to a protein, and (ii) an ssDNA DNAzyme engineered to cleave the aptamer in the bioaffinity sequence in the absence of protein–aptamer complex formation. As shown in Figure 1, bioaffinity adsorption of a protein biomarker onto the ssDNA aptamer will block the access of the DNAzyme to the cleavage site and prevent hydrolysis. To quantitatively measure the amount of protein blockage of DNAzyme cleavage activity, we attach an additional ssDNA sequence to the aptamer monolayer (labeled as a promoter–reporter sequence in Figure 1). If the aptamer–protein complex is not formed, then the DNAzyme will cut the ssDNA, removing the promoter–reporter sequence from the surface. Thus, the number of reporter–promoter sequences that remain on the surface is a measure of the number of adsorbed protein–aptamer complexes. This method of “protecting” the

Received: November 19, 2012

Published: January 27, 2013

DNAzyme cleavage site with the protein–aptamer complex is reminiscent of the process of enzymatic footprinting, in which binding sites for protein transcription factors are identified by the protection of dsDNA from DNA endonuclease activity by the formation of protein–dsDNA complexes.^{15,16}

As an initial demonstration, we have designed the two ssDNA oligonucleotides depicted in Figure 2: (i) a 98-base

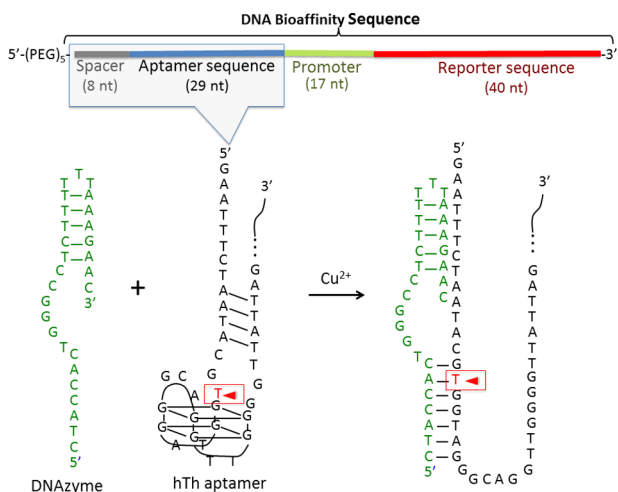


Figure 2. The DNAzyme sequence and the thrombin aptamer sequence as part of “bioaffinity sequence”. The red arrow indicates the DNAzyme cleaving site T₇.

“bioaffinity sequence” that consists of an 8 nucleotide spacer, a 29-base aptamer for the 37 kDa human thrombin protein (hTh)¹⁷ which has been used previously as a biomarker for various coagulation-related and cardiovascular diseases, a 17-base promoter sequence and a 40-base reporter sequence; and (ii) a 28-base ssDNA DNAzyme designed to cleave the thrombin aptamer at the thymine base position 7 in the aptamer sequence as shown in the figure. All sequences are listed in detail in the Supporting Information. As shown in the figure, the aptamer includes a G-quartet motif that interacts with hTh at the hTh-heparin binding exosite, leading to an aptamer–hTh binding energy of $\Delta G^\circ = -51.8$ kJ/mol at 25 °C.¹⁷ The design of the DNAzyme is based on a Cu²⁺-dependent DNA-cleaving deoxyribozyme reported by Breaker et al.¹⁸ In the presence of Cu²⁺ and ascorbic acid, this DNAzyme–substrate complex catalyzes a C4' oxidation at base T₇ of the aptamer sequence (see Figure 2).¹⁸ As shown in the figure, the DNAzyme is designed to bind to the aptamer sequence through a combination of a duplex and a triplex structure. The length of the duplex base-pairing sequence can be adjusted to vary the binding strength of the DNAzyme to the aptamer sequence.¹⁸ This 28-mer DNAzyme was designed to have a seven-base duplex structure with binding energy of $\Delta G^\circ \sim -43.1$ kJ/mol at 25 °C that is slightly less than the binding energy of the hTh–aptamer complex.

A set of gel electrophoresis measurements were used to demonstrate that the hTh protein can bind to the DNA aptamer and block DNAzyme cleavage activity in solution. Figure 3 is an electrophoresis gel image of a series of aliquots containing 1 μ M DNA bioaffinity sequence that were first incubated either with or without 1 μ M hTh, and then exposed to 2 μ M DNAzyme in solution (containing Cu²⁺ and ascorbic acid) for 1–36 h. The full image of the gel is provided in Supporting Information (Figure S1). The results clearly show

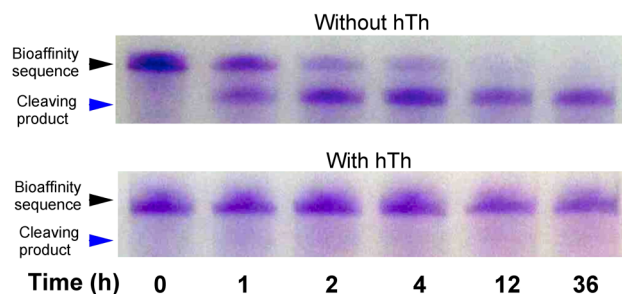


Figure 3. Time-based gel electrophoresis of DNAzyme footprinting in solution.

that in the absence of hTh, a significant amount of cleavage of the aptamer sequence was observed after 1 h, and complete cleavage of the aptamer was observed after 12 h. In contrast, in the presence of hTh, the aptamer remained uncleaved even after 36 h.

Having verified that the thrombin–aptamer complex can block DNAzyme activity in solution, we then used the DNAzyme footprinting methodology to detect thrombin with aptamer monolayers attached to gold thin films. As depicted in Figure 1, any thrombin–aptamer complex that blocks the DNAzyme cleavage activity will leave a promoter–reporter sequence on the surface. Thus, the fractional surface coverage of promoter–reporter sequences is a measure of the fractional surface coverage of adsorbed thrombin molecules (θ_{hTh}), which at low concentrations is proportional to the solution concentration (C_{hTh}): $\theta_{\text{hTh}} = K_{\text{ads}} \cdot C_{\text{hTh}}$ where K_{ads} is the Langmuir adsorption coefficient (1.2×10^8 M⁻¹ for hTh adsorption).¹⁰ The surface coverage of promoter–reporter sequences can be detected by various possible SPRI methods: (i) by direct SPRI detection of the hybridization adsorption of a complementary ssDNA sequence onto the monolayer, (ii) by SPRI detection of the adsorption of gold nanoparticles (AuNPs) modified with the complementary ssDNA sequence, or (iii) by NE-SPRI detection of RNA or DNA transcripts created in a surface polymerase reaction using the promoter–reporter sequence. We have verified that method (ii) can be used to detect thrombin at nanomolar concentrations (see Supporting Information for an exemplary experiment, Figure S2), and demonstrate here the most sensitive method (iii) to show that this DNAzyme footprinting technique can be used at extremely low relative surface coverages (down to $\theta_{\text{hTh}} = 10^{-5}$), corresponding to subpicomolar thrombin concentrations.

To detect the promoter–reporter sequences at these low surface coverages, we have employed an on-chip RNA amplification–detection strategy that we have used previously to detect ssDNA at femtomolar concentrations.¹² The on-chip enzymatic amplification process is depicted schematically in Figure 4a. As seen in the figure, the DNA bioaffinity sequence is immobilized onto an SPRI microarray element (denoted as a generator element (G)). A surface RNA polymerase reaction is used to create multiple RNA transcripts of the 40-mer reporter sequence (approximately 2000 copies as measured previously).¹² The transcribed RNA diffuses and adsorbs onto an adjacent SPRI microarray element (denoted as a detector element (D)) modified with a capture sequence of 20-mer ssDNA which is complementary to half of the RNA sequence. The adsorbed RNA transcript is detected by the further adsorption of AuNPs coated with ssDNA that is complementary to the other 20 bases of the RNA. This three-sequence

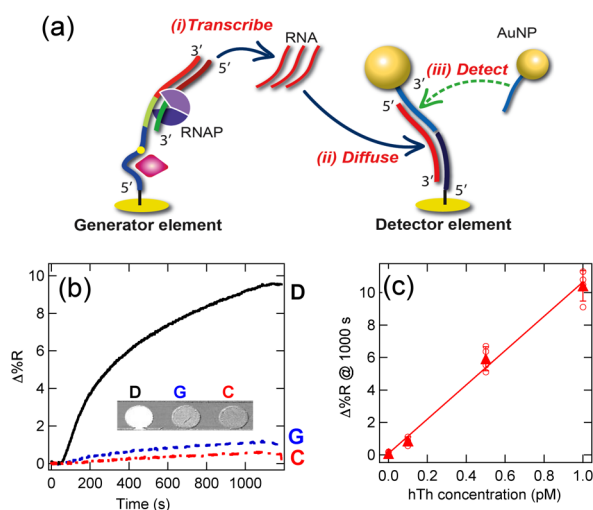


Figure 4. (a) Schematic diagram of transcription amplification and AuNP-enhanced SPRI from an uncleaved bioaffinity sequence. (b) SPRI real-time binding data of AuNPs adsorbed onto detector (D), generator (G) and control (C) microarray elements from a 1 pM hTh sample. (c) $\Delta\%R$ increase measured at 1000 s for AuNP adsorption onto detector microarray elements as a function of hTh concentration. The triangles indicate the average value from a set of microarray elements (hollow circles). A linear concentration dependence was observed with a detection limit of 100 fM.

hybridization assembly greatly enhances the SPRI signal from the detector elements.¹²

Figure 4b plots the SPRI real-time binding curves for the final step in this DNAzyme footprinting experiment with enzymatic amplification detection: the adsorption of ssDNA-modified AuNPs (2 nM) onto a microarray containing detector (D), generator (G) and control (C) elements. (The full SPRI difference image for this experiment is shown in Figure S3.) Prior to this step, the microarray was exposed to (i) a 1 pM hTh solution for 12 h, (ii) 0.2 μ M DNAzyme solution for 12 h, and finally (iii) an RNA polymerase solution (containing both the enzyme and ribonucleotides) for 2 h. The ssDNA sequences for the microarray elements are listed in Table S1. A very large $\Delta\%R$ increase of $\sim 10\%$ is observed from the Detector element after 1000 s. A small amount of AuNP adsorption ($\sim 1\%$) is also observed on the Generator elements, but this signal does not interfere with the quantitation of the Detector element signal. A small $\Delta\%R$ increase of less than 0.5% is observed from the Control elements, indicating very little nonspecific adsorption of the AuNPs onto these microarrays.

Figure 4c plots the $\Delta\%R$ increase measured for AuNP adsorption to the microarray detector element after 1000 s for a series of SPRI experiments at different hTh concentrations from 0 to 1 pM. A linear slope for $\Delta\%R$ was observed for hTh concentrations below 1 pM. A limit of detection of $\Delta\%R = 0.7\%$ corresponding to an hTh concentration of 100 fM was observed; at this concentration the hTh–aptamer complex surface coverage θ_{hTh} is equal to 10^{-5} . To detect this very low surface coverage, the DNAzyme footprinting method must be very effective at cleaving all of the unblocked aptamers in the monolayer, leaving only one intact hTh–aptamer complex for every 10 000 aptamer sequences on the surface. Above 1 pM, the $\Delta\%R$ continues to increase but saturates at 25% at approximately 100 pM (a complete $\Delta\%R$ plot for hTh concentrations from 0.1 pM to 1 nM on a logarithmic

concentration scale is shown in Figure S4). We attribute this saturation to the formation of a full AuNP monolayer on the Detector element as observed in previous NE-SPRI experiments.¹³ This saturation can be avoided by simply reducing the RNA transcription time (and thus the amount of enzymatic amplification), but it would also decrease the signal at the lower (subpicomolar) concentrations.

The initial experiments described in this letter have demonstrated that process of DNAzyme footprinting is a highly sensitive process for the detection protein–aptamer complexes in a surface bioaffinity sensing format. The use of DNAzyme footprinting with aptamer microarrays for the detection of proteins has several advantages as compared to the use of secondary enzyme-coupled antibodies with antibody microarrays. Conventional enzymatic amplification methods typically require two separate biorecognition sites on protein biomarkers for immobilization and signal enhancement.^{19–21} Moreover, the binding affinity of the DNAzyme to the substrate can be designed and tested by the stem-base pairing and the specific base pair sequence can also be modified.¹⁸ Additionally, the DNAzyme is relatively inexpensive, straightforward to handle, and less prone to nonspecific adsorption onto the microarray surface as compared with DNase I or other protein enzymes. A current limitation of the DNAzyme footprinting methodology is that the DNAzyme cleavage reaction is slow. For our protein biosensing measurements, we allowed the DNAzyme to react for 12 h with the microarray surface to be absolutely sure that all unprotected ssDNA were removed from the surface. Further experiments are needed to optimize the DNAzyme reaction conditions and reduce this reaction time. This DNAzyme footprinting methodology can be potentially expanded to a multiplexed platform by using multiple aptamers each with a distinct reporter sequence.²² Finally, we note that in addition to SPRI, the use DNAzyme footprinting for the detection of aptamer–protein complexes can be incorporated into any number of surface-based bioaffinity measurements (e.g., fluorescence imaging, LSPR spectroscopy, microring resonators, QCM, etc.).

■ ASSOCIATED CONTENT

Supporting Information

Experimental methods, supporting table and figures. This material is available free of charge via the Internet at <http://pubs.acs.org>.

■ AUTHOR INFORMATION

Corresponding Author

rcorn@uci.edu

Notes

The authors declare no competing financial interest.

■ ACKNOWLEDGMENTS

This work is supported by the National Institute of Health (2RO1 GM059622) and the University of California Cancer Research Coordinating Committee (CRCC). The authors thank Prof. Andrej Luptak and Cassandra Burke at University of California-Irvine for helpful discussions, as well as Dr. Kohei Nakamoto for graphical design.

■ REFERENCES

- (1) Vasan, R. S. *Circulation* **2006**, *113*, 2335–2362.

(2) Shi, M.; Bradner, J.; Hancock, A. M.; Chung, K. A.; Quinn, J. F.; Peskind, E. R.; Galasko, D.; Jankovic, J.; Zabetian, C. P.; Kim, H. M.; Leverenz, J. B.; Montine, T. J.; Ghingina, C.; Kang, U. J.; Cain, K. C.; Wang, Y.; Aasly, J.; Goldstein, D.; Zhang, J. *Ann. Neurol.* **2011**, *69*, 570–580.

(3) Rissin, D. M.; Kan, C. W.; Campbell, T. G.; Howes, S. C.; Fournier, D. R.; Song, L.; Piech, T.; Patel, P. P.; Chang, L.; Rivnak, A. J.; Ferrell, E. P.; Randall, J. D.; Provuncher, G. K.; Walt, D. R.; Duffy, D. C. *Nat. Biotechnol.* **2010**, *28*, 595–U25.

(4) Lockhart, D. J.; Winzeler, E. A. *Nature* **2000**, *405*, 827–836.

(5) Ng, E. W. M.; Shima, D. T.; Calias, P.; Cunningham, E. T.; Guyer, D. R.; Adamis, A. P. *Nat. Rev. Drug Discovery* **2006**, *5*, 1474–1776.

(6) Li, Y.; Lee, H. J.; Corn, R. M. *Anal. Chem.* **2007**, *79*, 1082–1088.

(7) Cho, E. J.; Collett, J. R.; Szafranska, A. E.; Ellington, A. D. *Anal. Chim. Acta* **2006**, *564*, 82–90.

(8) Eickhoff, H.; Konthur, Z.; Lueking, A.; Lehrach, H.; Walter, G.; Nordhoff, E.; Nyarsik, L.; Büssow, K.; Springer: Berlin/Heidelberg: 2002; Vol. 77, pp 103–112.

(9) Halpern, A. R.; Nishi, N.; Wen, J.; Yang, F.; Xiang, C. X.; Penner, R. M.; Corn, R. M. *Anal. Chem.* **2009**, *81*, 5585–5592.

(10) Zhou, W.-J.; Halpern, A. R.; Seefeld, T. H.; Corn, R. M. *Anal. Chem.* **2011**, *84*, 440–445.

(11) Gifford, L. K.; Sendroiu, I. E.; Corn, R. M.; Luptak, A. *J. Am. Chem. Soc.* **2010**, *132*, 9265–9267.

(12) Sendroiu, I. E.; Gifford, L. K.; Luptak, A.; Corn, R. M. *J. Am. Chem. Soc.* **2011**, *133*, 4271–4273.

(13) Zhou, W.-J.; Chen, Y.; Corn, R. M. *Anal. Chem.* **2011**, *83*, 3897–3902.

(14) Goodrich, T. T.; Lee, H. J.; Corn, R. M. *J. Am. Chem. Soc.* **2004**, *126*, 4086–4087.

(15) Hampshire, A. J.; Rusling, D. A.; Broughton-Head, V. J.; Fox, K. R. *Methods* **2007**, *42*, 128–140.

(16) Galas, D. J.; Schmitz, A. *Nucleic Acids Res.* **1978**, *5*, 3157–3170.

(17) Tasset, D. M.; Kubik, M. F.; Steiner, W. J. *Mol. Biol.* **1997**, *272*, 688–698.

(18) Carmi, N.; Breaker, R. R. *Bioorgan. Med. Chem.* **2001**, *9*, 2589–2600.

(19) Gorris, H. H.; Walt, D. R. *J. Am. Chem. Soc.* **2009**, *131*, 6277–6282.

(20) Sim, H. R.; Wark, A. W.; Lee, H. J. *Analyst* **2010**, *135*, 2528–2532.

(21) Tang, L.; Liu, Y.; Ali, M. M.; Kang, D. K.; Zhao, W.; Li, J. *Anal. Chem.* **2012**, *84*, 4711–4717.

(22) Chen, Y.; Nakamoto, K.; Niwa, O.; Corn, R. M. *Langmuir* **2012**, *28*, 8281–8285.